An asymmetric compliant antagonistic joint design for high performance mobility

CONFERENCE PAPER *in* PROCEEDINGS OF THE ... IEEE/RSJ INTERNATIONAL CONFERENCE ON INTELLIGENT ROBOTS AND SYSTEMS. IEEE/RSJ INTERNATIONAL CONFERENCE ON INTELLIGENT ROBOTS AND SYSTEMS · NOVEMBER 2013

DOI: 10.1109/IROS.2013.6697155

2013 IEEE/RSJ International Conference on
Intelligent Robots and Systems (IROS)
November 3-7, 2013. Tokyo, Japan

An Asymmetric Compliant Antagonistic Joint Design for High Performance Mobility

N.G.Tsagarakis, S.Morfey, H. Dallali, G.A Medrano-Cerda, and D.G. Caldwell

Abstract— **This paper presents the design of a novel compliant joint for high performance mobility. The design principle of the joint is based on an asymmetric compliant antagonistic scheme which is actuated by two motors of different power capability and efficiency. Torques from the two motors are transmitted to the joint through two elastic elements of different stiffness and energy storage capacity. The proposed compliant joint design combines high power performance, large energy storage capacity and physical resilience all necessary features for performing high performance mobility such as agile locomotion. The paper introduces the principle of operation, the design and mechanical implementation of the joint. Preliminary experimental trials demonstrate the joint performance in a single degree of freedom leg prototype system.**

I. INTRODUCTION

Despite the wide range of actuation systems developed in the past years, the lack of an actuation unit which can reach the functional performance of the biological actuation still remains the most significant barrier for the development of robots which can match the motion performance, energy efficiency and physical robustness of biological systems.

Compliant actuation systems have gained a lot of attention during the past 15-20 years and a diverse range of compliant joint designs have been realized. Their operation principles range from the original series elastic actuation (SEA) concept [1] to the most recent developments on variable impedance actuation (VIA) implementations [2], [3], [4], [5], [6], [7], [8], [9], [10], [11], [12]. The introduction of passive elasticity in robotic systems can improve their performance during interactions, provides energy storage capabilities [13] which potentially can increase their efficiency [14], [15] and peak power capacity and ultimately makes these robots more robust and less vulnerable to damages during impacts. Some of these advantages have been studied and validated in many works including the effect on safety during interaction [3], [16] the mechanical robustness and the generation of explosive motions with high power peaks [17], [18]. It is also evident that the energy storage capacity of the actuator can strongly affect its energetic efficiency. Conventional stiff actuated robots cannot elastically store and release energy, thus require large actuators and significantly more energy to execute their motions. On the other hand compliant actuators (fixed or variable stiffness) can store energy during a motion phase and then release it back in a another phase of the trajectory reducing the energy consumption and improving efficiency. The work in [14] studied the energic benefits in a single variable stiffness joint by exploiting the natural dynamics of the system. However, despite the big expectations of the research community, these energetic benefits have not yet demonstrated in multi-degree of freedom compliant actuated robots. There are two main difficulties in validating the latest. Firstly, how to achieve energetic efficient motion regulation for multi-dof compliant robots is not yet well understood at the control/trajectory generation level. Besides, at the hardware level the energy storage capacity of the existing compliant actuation implementations is very limited with the best performing system [19] able to only store energy of few Joules. Considering the higher mass and inertia of these compliant actuators (due to additional components required for the implementation of the passive compliance property), the increased frictional losses, and the damping control actions required to suppress oscillation and regulate their motion their energetic efficiency performance can be in question. This paper presents a novel compliant joint for high performance mobility. In contrary to the existing implementations of compliant actuators of fixed or variable compliance the proposed design is based on an arrangement that can be described as an antagonistic scheme characterized by high design asymmetry in the agonistic and antagonistic actuators and their elastic transmission systems. According to this design principle , Fig. 1(b), each branch (agonistic or antagonistic) provides specific functionality and performance with one branch providing high power motion capability and the other serving as an energy storage module. In overall the joint exhibits high power and energy storage density which is combined with physical robustness against interactions and impacts: all necessary for achieving high performance mobility. The rest of the paper is structured as follows. Section II presents the specifications and the functional principle of the high performance joint. Section III presents the mechanics of the joint while Section IV discusses the preliminary experimental results. Finally, the work concludes in Section V.

N.G.Tsagarakis, S.Morfey, H.Dalalli, G.M. Medrano-Cerda and D.G. Caldwell are with the Department of Advanced Robotics , Istituto Italiano di Tecnologia, Via Morego 30, 16163, Italy, nikos.tsagarakis at iit.it

II. DEVELOPMENT OF HIGH PERFORMANCE JOINT

A. Specifications

The goal of this work is to develop a high performance robotic joint which is capable of producing high power dynamic motions, demonstrating efficiency and physical robustness. This yields to the following desired features:

- High peak power and high power density.
- Excellent dynamic and high power motion performance.

- Large energy storage capacity and density.
- Efficient and quasi-controllable energy storage and release.
- Intrinsic and active regulated elasticity.
- Excellent physical robustness against perturbations and impacts.
- Full state measurement (position and torque) through the use of high resolution absolute position sensing.

The functional principle of the joint and the mechanical design adopted to achieve the above specifications are presented in the following sections.

B. Functional principle

The functional principle of the proposed joint is based on a compliant antagonistic scheme. A schematic representation of the joint arrangement is shown in Fig. 1(a). The joint configuration can be considered as a particular antagonistic scheme variant that is characterized by high asymmetry in the agonistic and antagonistic actuators which are dedicated to provide specific functionality and performance, Fig. 1(b). The first branch which, is called Power branch (PB), is a rotational drive based on a series elastic actuation unit that consists of a high power motor drive M_1 in series with a passive elastic transmission system SE. The elastic element in this branch serves three purposes. It firstly provides a bi-directional coupling between drive M_1 and the output link transmitting torques, secondly provides a decoupling functionality acting as a protection means for drive M_1 during high force impacts and finally through the monitoring of its deflection, is used as sensor which measures the torque delivered to the joint by drive M_1.

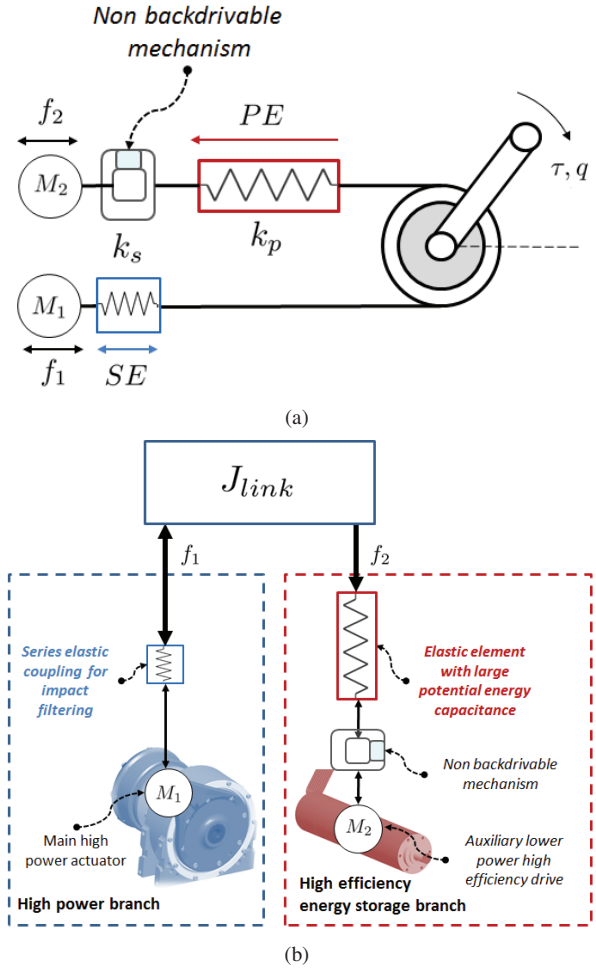

Fig. 1: High performance joint principle. a) Asymmetric antagonistic actuation scheme b) High power and large energy storage branch division.

The second branch is called Energy storage branch (ESB) and is based on a linear series elastic drive which consists of three main components. Drive M_2 is made off a lower power motor combined with a low reduction efficient linear transmission system. Forces generated by M_2 are transmitted to the joint through the elastic element PE. A particular characteristic of this elastic component and main difference with the elastic element of the other branch SE is its ability to store a large amount of energy, effectively acting as a potential energy capacitor.

Charging of the PE can be achieved in two ways. From the joint side the link kinetic or gravitational potential energy can be stored and released into the PE on the basis of the motion trajectory and system dynamics. Additionally, energy can be stored into the spring using drive M_2 with this actuator in this case acting as a tensioning drive. To achieve efficient regulation and maintenance of the PE pretension motor M_2 combines the low friction and highly backdrivable linear transmission system with a non backdrivable transmission component implemented using a two side acting overrunning clutch mechanism that is placed between motor M_2 and the elastic transmission. This prevents the reverse transmission of motion from the elastic element PE side after the pretension has been set, eliminating the need for continuously supporting the pretension of the PE from drive M_2.

III. Mechanics of the Joint

To evaluate the performance of the joint principle described above, we developed a single DOF prototype leg system Fig. 2. The specification of high peak power and high power density combined with excellent high dynamic and high power motion performance can only be achieved with the use of high performance components and substantial design effort to optimize the overall size and weight of the joint. Both actuators are positioned high on the leg to minimize the inertia of the leg and to reduce the distance of the centers of mass of the leg links, enabling lower power consumption for dynamic movements. Structural elements are made from carbon fiber, chosen for its excellent strength-to-weight ratio reducing the total mass without compromising structural rigidity.

A. Power branch (PB)

The Power Branch consists of a frameless brushless DC motor, a Harmonic Drive gearbox with reduction 80:1 and a flexible torsion bar between the gearbox and the motor

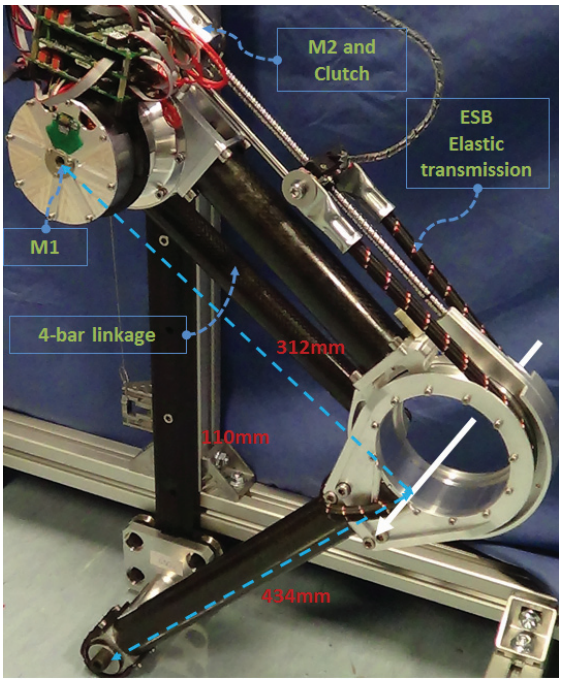

Fig. 2: Physical prototype of the joint.

output, Fig. 3(a). The motor is a custom-specifications high performance motor based on an optimized design that results in higher winding conductor volume. Special winding insulation with high-temperature superior electrical properties provides improved breakdown strength and resistivity at high temperatures permitting the motor to function continues at temperatures up to 220°C. At 150°C the motor can deliver $900W$ of continuous power and has a peak power capability of $2.8KW$. The motor is equipped with three position sensors allowing for full state feedback control of the actuator. In detail, an incremental optical encoder (MicroE Optical encoder with 12-bit of resolution) is mounted at the motor side before gear box, one relative magnetic encoder (Austria Microsystems with 19-bit of resolution) monitors the position of M_1 after the harmonic reduction drive while an additional 19-bit absolute encoder measures the angle of the link after the flexible torsion bar. The torque provided by motor M_1 is monitored through the measurement of the deflection of the torsional bar by means of the two 19-bit bit encoders reported above, Fig. 3(a). The stiffness of the torsion bar was chosen to be $K_s = 950Nm/rad$ which gives a torque measurement resolution of $15mNm$.

The overall weight of the power branch motor, Fig. 3(b) is approximately $1.7Kg$. The power from M_1 is transferred to the knee by an inelastic four-bar linkage,Fig. 2 with a 1:1 velocity ratio.

B. Energy storage branch (ESB)

One of the desired characteristics of the Energy storage branch (ESB) is the ability to store large amount of energy effectively acting as a potential energy capacitor. High energy storage capacity implies the integration of elastic elements that are able to store large amounts of energy. Mechanical metal springs tend to be big and substantially heavy, which can increase significantly the overall size, weight and reduce the power density. This is obviously in contradiction to the overall design objectives of this joint. To maximize the energy storage capacity of the ESB while maintaining low weight and compactness we consider in this implementation a type of an elastic band similar to shock cords. This flexible cord is made of a number of elastic strands which are enclosed inside a woven braided cotton sheath. The sheath does not extend elastically, but it is braided with its strands spiraling around the core so that a longitudinal pull causes it to squeeze the core, transmitting the core's elastic compression to the longitudinal extension of the sheath and cord. Another important aspect of the ESB is the capability to regulate the pre-tension of this elastic element allowing to continuously and selectively engage the elastic element and control the energy storage during the joint motion. This is achieved through a variable pretension

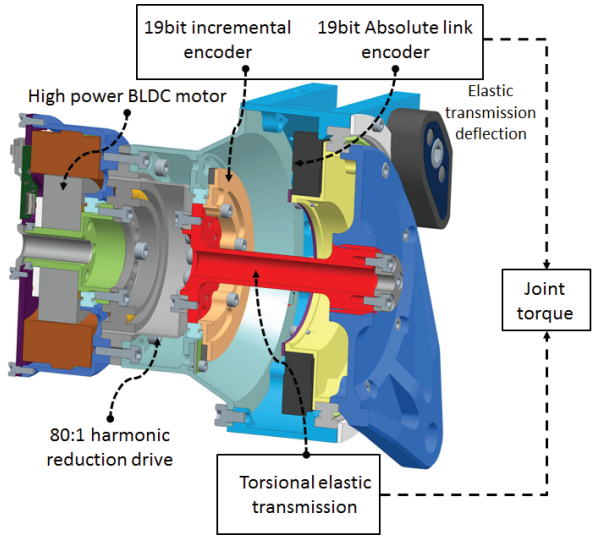

(a)

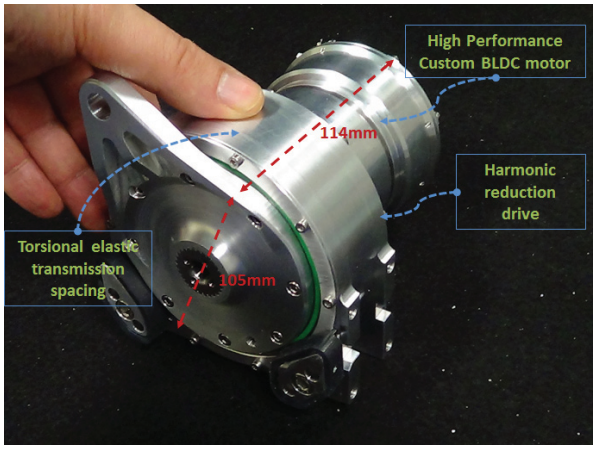

(b)

Fig. 3: High Power branch drive. a) Cross section of the main motor CAD assembly b) Physical prototype of the high power branch motor.

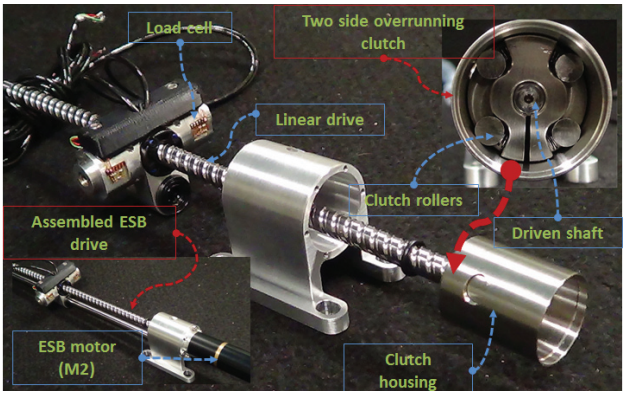

Fig. 4: Prototype of the energy storage branch drive.

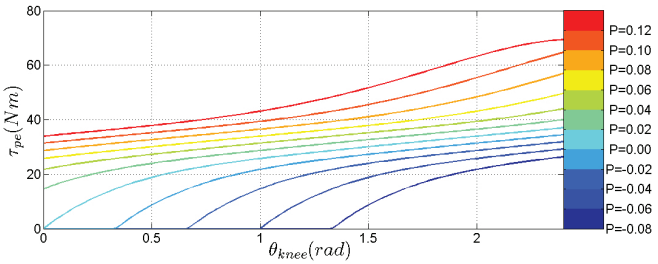

Fig. 5: Torque produced at the joint by the PE.

mechanism which uses the linear drive shown in Fig. 4. This linear drive is composed of a brushless DC servomotor (Maxon EC 22, 100W) coupled to a planetary gearhead with 29:1 reduction and peak torque of 3Nm. The gearhead output drives a highly backdrivable ball screw transmission (pitch of 10mm). Given the performance of M_2 the pitch of the ball screw was selected to permit the full pretension $(0.12m)$ of the elastic element within $1sec$. To achieve efficient regulation and maintenance of the PE pretension without overloading motor M_2 the backdrivable ball screw transmission is combined with a two-way overrunning clutch module which implements the non-backdrivable mechanism of Fig. 1(b). The clutch prevents the backdriving (with no significant losses) of the ball screw from the elastic element PE after the pretension has been set, eliminating the need for continuously supporting the pretension with motor M_2. The capability of adjusting the pretension of PE using drive M_2 gives to the joint superior flexibility of using the stored energy in different manners to minimize energy or to

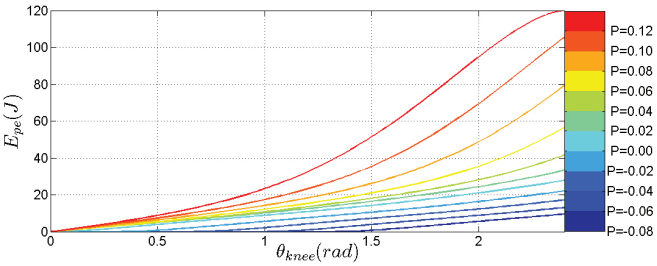

Fig. 6: Energy stored in the PE.

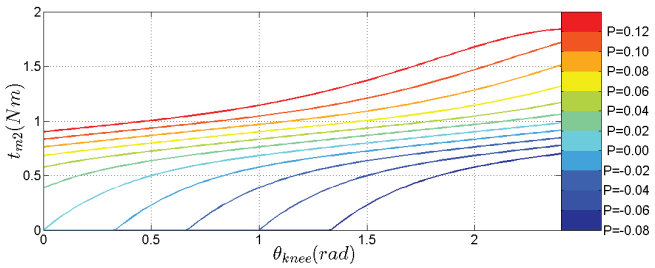

Fig. 7: Torque required by M2 to set the pretension.

generate peak power explosive motions. As an example, the Energy storage branch (ESB) can provide variable passive gravity compensation around a joint position by regulating the equilibrium of PE component or it can efficiently contribute to the joint torque generation in high-torque/low-speed motions. Figure 5 shows the torque delivered to the joint by the PE as function of the pretension p and the knee angle θ_{knee}. As it can be seen the PE elastic element exhibits an nonlinear force/pretension trend permitting also the regulation of the overall joint stiffness through the pretension p.

This torque can be used to assist the Power branch (PB) and reduce the energy required to achieve the motion (to mention here that the ball screw transmission system of motor M_2 is more efficient than the harmonic drive of motor M_1). Additionally it can work antagonistically with the Power branch (PB) to charge the PE prior to the generation of explosive motions in the reverse motion of the charging direction. Figure 6 presents the energy that can be stored in the PE as a function of the pretension p and the knee angle θ_{knee}. The torque requirements of the M_2 drive while performing the pretension of the PE elastic element are shown in Fig. 7.

It is evident that this unidirectional rubber type elastic element, which behaves as pre-loaded extension spring, can only apply torques τ_{pe} when it is stretched according to (1) below.

$$\tau_{pe} = \begin{cases} k_{pe}(p - rq) + d_{pe}(\dot{p} - r\dot{q}) & if\ p - rq < \quad 0 \\ 0 & if\ p - rq \geq \quad 0 \end{cases} \tag{1}$$

where k_{pe} and d_{pe} are the equivalent stiffness and damping constants of the elastic element PE, p is the pretension set by motor M_2, r is the radius of the knee joint pulley and q is the angle of the knee. Depending on the pretension p the elastic element PE will be engaged at a chosen knee angle and will start to generate torque to the knee joint. It is therefore clear that the above energy efficiency and power performance advantages are offered only to one direction of the joint motion(counter clockwise according to the schematic setup shown Fig. 1(a). This is compatible with the difference in strength and size observed also in the agonistic and antagonistic muscles in many joints of biological systems including humans.

The ESB drive additionally incorporates sensing for the measurement of the linear drive position (pretension) as well

as for the measurement of the tension of the elastic cord. This effectively permits the monitoring of the torque applied to the joint by the energy storage branch.

IV. Experimental results

Experiments were conducted with the single DOF leg prototype shown in Fig. 2 in order to evaluate the performance of the asymmetric compliant antagonistic joint. For this purpose, an impedance plus gravity compensation controller was implemented at the motor variables for regulating the motion of motor M_1. The reference for the inner torque loop was given by:

$$\tau_{ref} = K_p(\theta_d - \theta) + K_d(\dot{\theta_d} - \dot{\theta}) + g(\theta) - \tau_{pe} \quad (2)$$

where K_p and K_d represent the impedance stiffness and damping parameters respectively, θ_d is the desired motor position and θ is the motor position after the gearbox and before the elastic torsional transmission. Finally, $g(\theta)$

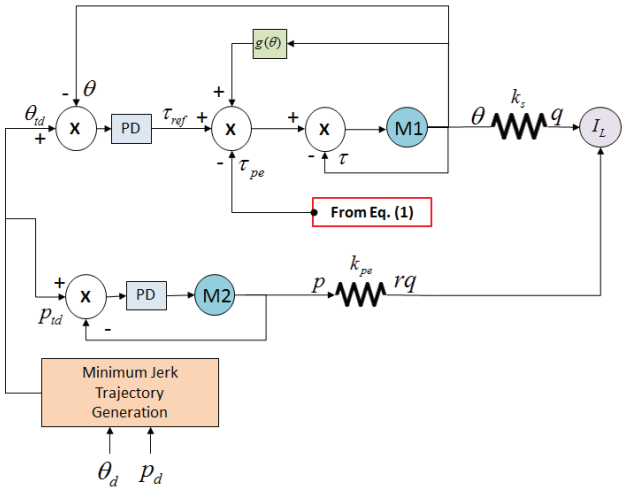

Fig. 8: The control diagram used in the experimental trials.

denotes the gravity computed based on the motor variable. To take into account the torque generated by the ESB according to (1) τ_{pe} is subtracted to derive the torque demand for motor M_1.

For the second motor M_2 a standard proportional derivative controller (PD) was implemented for regulating the pretension of the PE in the energy storage branch. The overall control scheme used in these trials is depicted in Fig. 8. The inputs are the desired position θ_d of motor M_1 and the desired pretension p_d of motor M_2. The minimum jerk trajectory block generates the reference inputs (θ_{td}, p_{td}) for the two motor controllers from the desired inputs (θ_d, p_d).

Both controllers were implemented on custom DSP-boards based on the Texas Instruments Luminary DSP chip LM3S8962. The control loop was executed at $1KHz$ while the communication with the host PC was achieved through a real time Ethernet link at the same rate of $1KHz$. These preliminary trials were carried out to validate the overall design and demonstrate the synergistic contribution of the two antagonistic branch on the delivery of the torque

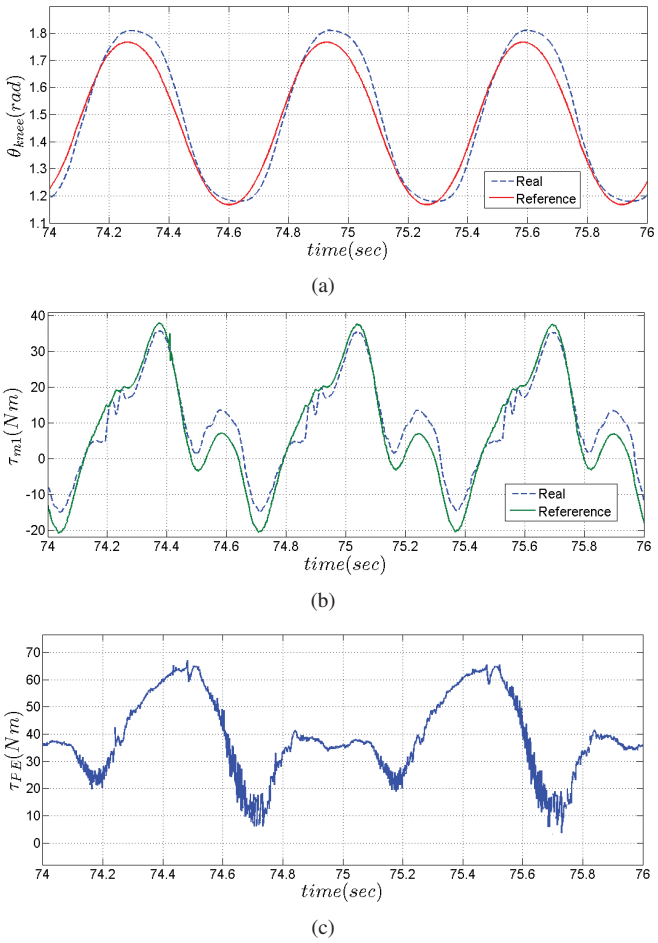

Fig. 9: Experimental data from the leg executing a sine reference of $1.5Hz$, a) Knee trajectory, b) Torque supplied by actuator $M1$ and c) Torque delivered by the ESB.

required to executed the reference motion. The leg was loaded with $10Kg$ of weight mounted above the hip level. It was then driven by a sinusoidal input θ_d at the frequency of $1.5Hz$. During this experiment the stiffness and damping parameters of the impedance controller for motor M_1 were set to $K_p = 70Nm/rad$ and $K_d = 3Nsec/rad$ respectively implementing a relatively soft motion behavior that permits interaction with the leg while executing this sinusoidal motion. Figure 9(a) presents the reference and the real knee trajectory tracked under these soft impedance settings. The torque delivered by the main actuator M_1 and the energy storage branch are also presented in Fig. 9(b) and Fig. 9(c) respectively clearly demonstrating the contribution of the ESB branch in the torque required for the execution of the motion. To note here that the amount of the torque generated by the ESB can be controlled through the pretension functionality as demonstrated in Fig. 5. In Fig. 10 snapshots of the leg during the execution of the experiment are presented showing the soft interaction performance of the leg prototype during perturbations applied by the operator. It can also be observed in the accompanied video that the leg demonstrates adequate robustness and ability to tolerate

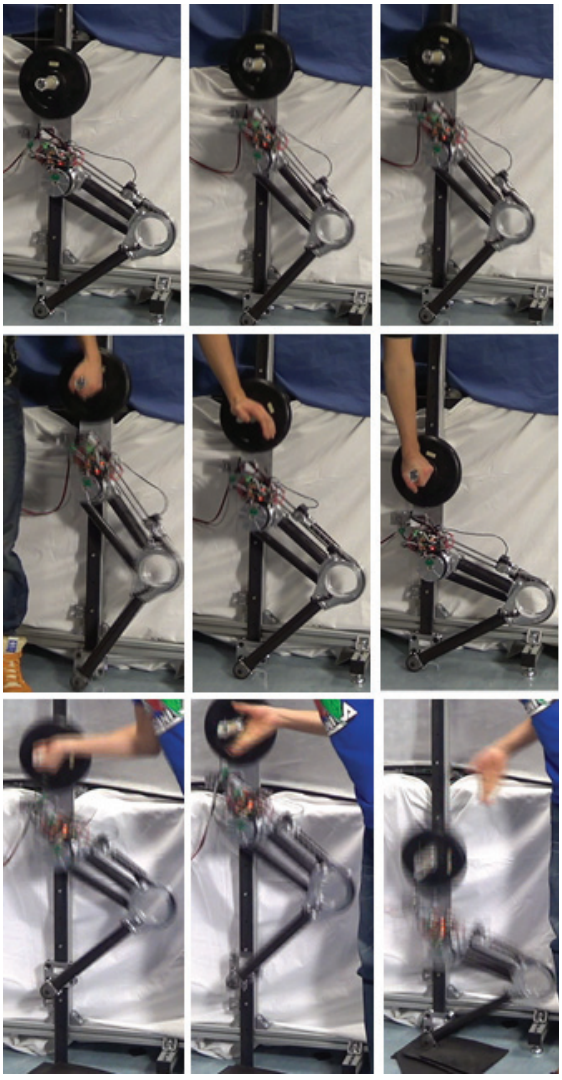

Fig. 10: Snapshots of the leg during the experiment.

these disturbances including falling impacts.

V. CONCLUSIONS

In this paper the functional principle, the design, and implementation of a novel antagonistic actuation scheme were presented. The unit is intended to be used for the development of high performance robotic systems which will demonstrate high power and large energy storage capacity. The proposed actuation unit is based on an asymmetric compliant antagonistic scheme powered by two motors. The torques from the two motors are transmitted to the joint through two elastic elements of different stiffness and energy storage capacity. The proposed compliant joint design combines high power performance, large energy storage capacity and physical robustness which are essential features for human-like high motion performance. After presenting its functional principle the joint was used to power a single degree of freedom leg prototype with preliminary experimental trials validating the joint functionality.

VI. ACKNOWLEDGMENT

This work is supported by the WALK-MAN FP7-ICT-2013-10 European Commission project.

REFERENCES

[1] Pratt G. and Williamson M. Series elastic actuators. *IROS*, page 399, 1995.

[2] T.G. Sugar. A novel selective compliant actuator. *Mechatronics*, 12(9):1157–1171, 2002.

[3] A. Bicchi, G. Tonietti, M. Bavaro, and M. Piccigallo. Variable stiffness actuators for fast and safe motion control. In *Int. Symposium Robotics Research*, pages 100–110, 2003.

[4] J. W. Hurst, J. E. Chestnutt, and A. Rizzi. An actuator with physically variable stiffness for highly dynamic legged locomotion. *ICRA*, pages 4662 – 4667, 2004.

[5] G. Tonietti, R. Schiavi, and A. Bicchi. Design and control of a variable stiffness actuator for safe and fast physical human/robot interaction. *ICRA*, pages 526–531, 2005.

[6] R. Van Ham, B. Vanderborght, M. Van Damme, B. Verrelst, and D. Lefeber. Maccepa, the mechanically adjustable compliance and controllable equilibrium position actuator: Design and implementation in a biped robot. *Robotics and Autonomous Systems*, 55(10):761–768, 2007.

[7] Sebastian Wolf and Gerd Hirzinger. A new variable stiffness design: Matching requirements of the next robot generation. In *IEEE International Conference on Robotics and Automation (ICRA 2008)*, pages 1741–1746, May 2008.

[8] Byeong-Sang Kim and Jae-Bok Song. Hybrid dual actuator unit: A design of a variable stiffness actuator based on an adjustable moment arm mechanism. In *Robotics and Automation (ICRA), 2010 IEEE International Conference on*, pages 1655–1660. IEEE, 2010.

[9] N.G. Tsagarakis, I. Sardellitti, and D.G. Caldwell. A new variable stiffness actuator (compact-vsa): Design and modelling. In *Intelligent Robots and Systems (IROS), 2011 IEEE/RSJ International Conference on*, pages 378–383. IEEE, 2011.

[10] M.G. Catalano, G. Grioli, M. Garabini, F. Bonomo, M. Mancinit, N. Tsagarakis, and A. Bicchi. Vsa-cubebot: a modular variable stiffness platform for multiple degrees of freedom robots. In *Robotics and Automation (ICRA), 2011 IEEE International Conference on*, pages 5090–5095. IEEE, 2011.

[11] Ludo C Visser, Raffaella Carloni, and Stefano Stramigioli. Energy-efficient variable stiffness actuators. *Robotics, IEEE Transactions on*, 27(5):865–875, 2011.

[12] A. Jafari, NG Tsagarakis, I. Sardellitti, and DG Caldwell. How design can affect the energy required to regulate the stiffness in variable stiffness actuators. In *Robotics and Automation (ICRA), 2012 IEEE International Conference on*, pages 2792–2797. IEEE, 2012.

[13] M. Laffranchi, NG Tsagarakis, F. Cannella, and DG Caldwell. Antagonistic and series elastic actuators: a comparative analysis on the energy consumption. In *Intelligent Robots and Systems, 2009. IROS 2009. IEEE/RSJ International Conference on*, pages 5678–5684. IEEE, 2009.

[14] A. Jafari, N.G. Tsagarakis, and D.G. Caldwell. Exploiting natural dynamics for energy minimization using an actuator with adjustable stiffness (awas). In *Robotics and Automation (ICRA), 2011 IEEE International Conference on*, pages 4632–4637. IEEE, 2011.

[15] B. Vanderborght, N.G. Tsagarakis, R. Van Ham, I. Thorson, and D.G. Caldwell. Maccepa 2.0: compliant actuator used for energy efficient hopping robot chobino1d. *Autonomous Robots*, 31(1):55–65, 2011.

[16] M. Laffranchi, NG Tsagarakis, and D.G. Caldwell. Safe human robot interaction via energy regulation control. In *Intelligent Robots and Systems, 2009. IROS 2009. IEEE/RSJ International Conference on*, pages 35–41. IEEE, 2009.

[17] M. Garabini, A. Passaglia, F. A. W. Belo, P. Salaris, and A. Bicchi. Optimality principles in variable stiffness control: the vsa hammer. In *IEEE IROS*, pages 3770 – 3775, 2011.

[18] M. Garabini, A. Passaglia, F. Belo, P. Salaris, and Bicchi. Optimality principles in stiffness control: The vsa kick. In *IEEE ICRA*, pages 3341–336, 2012.

[19] Sebastian Wolf, Oliver Eiberger, and Gerd Hirzinger. The dlr fsj: Energy based design of a variable stiffness joint. In *Robotics and Automation (ICRA), 2011 IEEE International Conference on*, pages 5082–5089. IEEE, 2011.